SPATIO-TEMPORALLY REGULARIZED 4-D CARDIOVASCULAR C-ARM CT RECONSTRUCTION USING A PROXIMAL ALGORITHM

Oliver Taubmann[1,2,*], *Mathias Unberath*[1,2,*], *Günter Lauritsch*[3], *Stephan Achenbach*[4], *Andreas Maier*[1,2]

[1] Pattern Recognition Lab, Friedrich-Alexander-University Erlangen-Nuremberg, Germany
[2] Erlangen Graduate School in Advanced Optical Technologies (SAOT), Germany
[3] Siemens Healthcare GmbH, Forchheim, Germany
[4] Department of Cardiology, Friedrich-Alexander-University Erlangen-Nuremberg, Germany
[*] These authors contributed equally to this work.

ABSTRACT

Tomographic reconstruction of cardiovascular structures from rotational angiograms acquired with interventional C-arm devices is challenging due to cardiac motion. Gating strategies are widely used to reduce data inconsistency but come at the cost of angular undersampling. We employ a spatio-temporally regularized 4-D reconstruction model, which is solved using a proximal algorithm, to handle the substantial undersampling associated with a strict gating setup. In a numerical phantom study based on the CAVAREV framework, similarity to the ground truth is improved from $82.3\,\%$ to $87.6\,\%$ by this approach compared to a state-of-the-art motion compensation algorithm, whereas previous regularized methods evaluated on this phantom achieved results below $80\,\%$. We also show first image results for a clinical patient data set.

Index Terms— Spatio-temporal regularization, Cardiovascular reconstruction, Total variation, C-arm CT

1. INTRODUCTION

Providing physicians with the 3-D anatomy of vascular trees is considered beneficial for diagnostic assessment and interventional guidance [1]. Consequently, reconstruction of coronary artery trees from C-arm CT rotational angiography has received considerable attention, particularly because it requires motion management to handle cardiac motion. Retrospective electrocardiogram (ECG) gating is commonly used but yields very few views of the same heart phase; often, only four to ten views are available. Symbolic reconstruction algorithms are capable of handling such situations [1, 2], yet typically do not provide information about the lumen and, thus, are not suitable for detecting stenoses.

In contrast, volumetric (tomographic) reconstruction can alleviate the aforementioned problems, but usually requires a sufficient amount of consistent data [1, 3, 4]. To this end, state-of-the-art methods seek to include images at different heart phases into the reconstruction process using motion correction and compensation strategies [2, 4–6]. Unfortunately, estimating the highly complex cardiac motion is challenging and computationally demanding.

Rather than compensating for motion, novel iterative reconstruction algorithms exploit image properties in spatial and, more importantly, temporal domain [7]. In addition to employing *spatial* regularizers used in compressed sensing such as (spatial) total variation (TV) minimization [3], these methods reconstruct images at multiple cardiac phases simultaneously while allowing for communication among them using *temporal* regularizers. Therefore, they implicitly address the problem of insufficient data more effectively [7].

In this paper, we use spatio-temporal regularization and a proximal optimization algorithm to reconstruct contrasted vasculature from rotational angiography sequences. In a numerical phantom study based on the CAVAREV platform [8], we demonstrate that the proposed approach outperforms state-of-the-art methods. Finally, we show qualitative results for a clinical patient data set.

2. METHODS

2.1. Vessel Extraction

Rotational angiograms suffer from severe truncation as conventional detectors are not large enough to fit projections of the entire thorax. However, the contrasted arteries lie in the central field of view and are, therefore, not truncated. To limit truncation-related artifacts in the reconstructions, we perform single-frame background subtraction as proposed in [9].

First, the contrasted vessels are segmented in projection domain using filters based on first- and second-order derivatives yielding binary segmentation masks. These masks are used to artificially corrupt the acquired projections with the aim of removing all evidence of contrast agent. Subsequently, a virtual background image is estimated via spectral deconvolution that, finally, is subtracted from the acquired projections yielding non-truncated, virtual digital subtraction angiograms (*vessel images*, cf. Fig. 1).

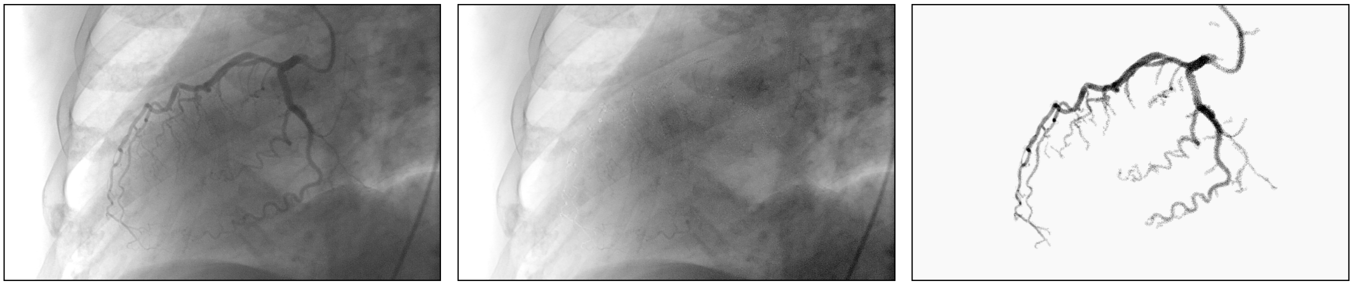

Fig. 1: A single frame taken from the rotational angiogram of a clinical patient (left), the corresponding inpainted background image (center), and the extracted vessel image (right).

2.2. Electrocardiogram Gating

The extracted vessel images are then retrospectively grouped into several subsets (*gates*) corresponding to individual cardiac phases, based on their relative position between two consecutive R-peaks in the ECG signal acquired during the scan. Typically, gating involves a trade-off: With wider windows, more data is available for each gate to be reconstructed [6]. However, this also leads to a larger amount of residual motion and, therefore, data inconsistency within each gate.

Our approach is to minimize residual motion by selecting, for any one gate, only the single best-matching image from each recorded heart cycle (*strict gating*). The resulting downside of a reduced amount of data per gate is compensated for by the use of temporal regularization (see section 2.3), which enables the exchange of information between all gates to overcome the problem of undersampling. To capitalize on this effect as much as possible, we choose the total number of gates such that (nearly) all available data is used.

2.3. Tomographic 4-D Reconstruction

We treat joint reconstruction of all gates as an optimization problem which consists in minimizing a cost function,

$$\underset{\boldsymbol{i}\in\mathbb{R}_+^N}{\operatorname{argmin}} \frac{1}{2}\|\boldsymbol{A}\boldsymbol{i}-\boldsymbol{p}\|_2^2 + \lambda_\mathrm{s}\|\boldsymbol{D}_\mathrm{s}\boldsymbol{i}\|_{1,2} + \lambda_\mathrm{t}\|\boldsymbol{D}_\mathrm{t}\boldsymbol{i}\|_1, \qquad (1)$$

where

- $\boldsymbol{i}$ is the vectorized form of the desired (non-negative) solution in the space of 4-D volumes,
- $\boldsymbol{A}$ is the system matrix encoding the scan geometry, relating $\boldsymbol{i}$ to the gated vessel images vectorized in $\boldsymbol{p}$,
- λ_s, λ_t are weights associated with the sum of the spatial image gradient magnitudes $\|\boldsymbol{D}_\mathrm{s}\boldsymbol{i}\|_{1,2}$ (spatial TV) and the sum of the absolute values of the temporal image gradients $\|\boldsymbol{D}_\mathrm{t}\boldsymbol{i}\|_1$ (temporal TV), respectively. All gradients are computed using simple forward differences.

An efficient proximal primal-dual splitting algorithm for solving this type of problem, which is made up of both differentiable and non-differentiable components, was proposed by Condat [10]. Applying Algorithm 1 from [10] to our task, we obtain the updates,

1. $\boldsymbol{i} \leftarrow \left(\boldsymbol{i} - \tau(\boldsymbol{A}^\top(\boldsymbol{A}\boldsymbol{i}-\boldsymbol{p}) + \boldsymbol{D}_\mathrm{s}^\top\boldsymbol{g}_\mathrm{s} + \boldsymbol{D}_\mathrm{t}^\top\boldsymbol{g}_\mathrm{t})\right)_+$, which is the primal update step with step length τ, the dual variables $\boldsymbol{g}_\mathrm{s}$ and $\boldsymbol{g}_\mathrm{t}$ corresponding to the spatial and temporal gradients, respectively, and the element-wise non-negativity constraint $(\cdot)_+ : i \mapsto \max\{i, 0\}$,
2. $\boldsymbol{g}_\mathrm{s} \leftarrow \operatorname{prox}_{\sigma(\lambda_\mathrm{s}\|\cdot\|_{1,2})^*}(\boldsymbol{g}_\mathrm{s} + \sigma\boldsymbol{D}_\mathrm{s}(2\boldsymbol{i}-\boldsymbol{i}_\mathrm{prev}))$, which is the dual update step for $\boldsymbol{g}_\mathrm{s}$ with step length σ and the element-wise proximal operator $\operatorname{prox}_{\sigma(\lambda_\mathrm{s}\|\cdot\|_{1,2})^*} : \boldsymbol{v} \mapsto \boldsymbol{v}/\max\{\|\boldsymbol{v}\|_2/\lambda_s, 1\}$, where $\boldsymbol{i}_\mathrm{prev}$ denotes the value of $\boldsymbol{i}$ from the previous iteration,
3. $\boldsymbol{g}_\mathrm{t} \leftarrow \operatorname{prox}_{\sigma(\lambda_\mathrm{t}\|\cdot\|_1)^*}(\boldsymbol{g}_\mathrm{t} + \sigma\boldsymbol{D}_\mathrm{t}(2\boldsymbol{i}-\boldsymbol{i}_\mathrm{prev}))$, which is the dual update for $\boldsymbol{g}_\mathrm{t}$ with step length σ and the proximal operator $\operatorname{prox}_{\sigma(\lambda_\mathrm{t}\|\cdot\|_1)^*} : g \mapsto g/\max\{|g|/\lambda_t, 1\}$.

Iterating this update sequence with step lengths τ, σ chosen such that $\tau\left(\beta/2 + \sigma\|\boldsymbol{D}_\mathrm{s}^\top\boldsymbol{D}_\mathrm{s} + \boldsymbol{D}_\mathrm{t}^\top\boldsymbol{D}_\mathrm{t}\|\right) < 1$, where β is the Lipschitz constant of the data-fidelity term $\frac{1}{2}\|\boldsymbol{A}\boldsymbol{i}-\boldsymbol{p}\|_2^2$, is proven to converge to an optimal solution of Eqn. 1 [10].

2.4. Experiments

2.4.1. Phantom Study

Quantitative assessment of image quality is carried out using CAVAREV [8], a platform for evaluating cardiac vasculature reconstruction. It is based on a dynamic numerical phantom derived from actual patient data, projections of which are simulated using the calibrated acquisition geometry of a real C-arm system. It covers seven heart cycles over 133 projection images. As we assume a breathhold protocol, we use the variant without respiratory motion. We reconstruct 19 $(= 133/7)$ gates on a 256^3 grid with an isotropic voxel size of $0.5\,\mathrm{mm}$. Feasible weights λ_s, λ_t are determined in a grid search.

CAVAREV repeatedly binarizes the reconstructed volume image to be evaluated with a sweeping threshold and compares it to segmentation masks of the ground-truth morphology in all motion states using the Dice similarity coefficient

Table 1: Best Dice coefficients achieved in CAVAREV [8]. Methods are listed in ascending order w. r. t. their scores.

Method	Dice Score
Standard FDK	0.431
ECG-Gated FDK	0.595
Dynamic Level Sets [11]	0.692
PICCS [3, 12]	0.726
L1 minimization [3, 13]	0.730
Streak-Reduced ECG-Gated FDK [6]	0.744
Residual Motion Compensation [4]	0.776
Spatial Total Variation [3]	0.785
Motion Compensation [6]	0.823
Spatio-temporal TV (proposed)	**0.876**

[8], a common two-sided measure for the overlap of two binary images ranging from zero (no overlap) to one (perfect match). As the final score, it selects the best value over all thresholds and motion states. Scores for several state-of-the-art methods have been published (cf. Tab. 1). We state the best 3-D score obtained with any of the reconstructed gates to ensure comparability with previously reported scores. This is appropriate as, unlike inherently 3-D methods, no specific cardiac phase has to be pre-selected in our method; all gates, including the best, are readily available after reconstruction.

2.4.2. Clinical Data

In order to assess applicability of our method to real-world scans, we test it on a clinical patient data set acquired with an *Artis one* system (Siemens Healthcare GmbH, Forchheim, Germany). It covers five heart cycles over 133 projections during a 4 s rotation. We reconstruct 27 ($\approx 133/5$) gates on a 256^3 grid with an isotropic voxel size of 0.5 mm. As no ground truth is available, qualitative evaluation is carried out by visual inspection of the results.

3. RESULTS AND DISCUSSION

3.1. Phantom Study

The proposed method has its maximum Dice coefficient of 0.876 for the gate corresponding to a relative heart phase of $18/19 \approx 95\,\%$. This score is the highest one achieved in CAVAREV at the time of writing (cf. Tab. 1). A volume rendering of the corresponding image is shown in Fig. 3a. Some parts of the cardiac cycle are comparatively more difficult to reconstruct (Fig. 2, top) as they contain more motion. This is in line with what has been observed in prior work [3]. Having surpassed methods using spatial TV regularization [3] or motion compensation [6] in fewer than 200 iterations, the improvement in image quality gradually starts to level out as the optimization converges (Fig. 2, bottom).

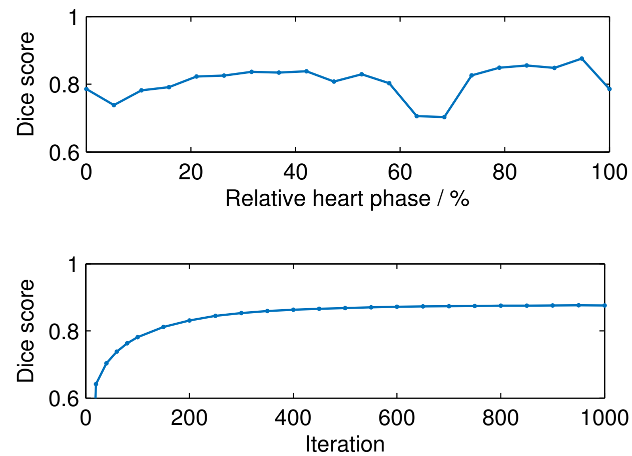

Fig. 2: Dice coefficients for the CAVAREV phantom study over all gates (top) and over all iterations for the best gate at $\approx 95\,\%$ relative heart phase (bottom).

3.2. Clinical Data

The image reconstructed from the clinical patient data is visualized in Fig. 3b. In contrast to the phantom, this data set contains a considerable amount of noise as well as respiratory motion, albeit little, and comprises only four or five views per gate. Even so, barring residual motion artifacts in the proximal region, the obtained results exhibit good image quality.

Some distal vascular structures are not fully recovered due to the fact that in several frames, the vessel tree is not completely recognized by the extraction step (section 2.1), leading to inconsistent data. A mild example of this issue can be seen in Fig. 1, where parts of a single vessel are still visible in the lower part of the inpainted background image. Overall, the employed regularization scheme appears to be robust when dealing with such inconsistencies. The benefit of temporal regularization becomes apparent when comparing Fig. 3b to Fig. 3c, which is obtained using spatial regularization only while all other parameters are left unchanged. It suffers from an increased amount of noise and artifacts and partially fails to resolve structures that are clearly discernible in Fig. 3b.

4. CONCLUSION AND OUTLOOK

A novel approach to dynamic tomographic reconstruction of cardiac vasculature from rotational angiograms is presented. Based on the key idea of minimizing residual motion within each gate while, at the same time, exploiting all available data by means of spatio-temporal regularization, it outperforms both algebraic and analytical state-of-the-art techniques previously evaluated in the considered numerical phantom framework. This suggests that relying on a sparsity-based 4-D image model is a viable alternative to the use of smooth motion models such as B-Splines, which are common in motion-compensated reconstruction methods [6].

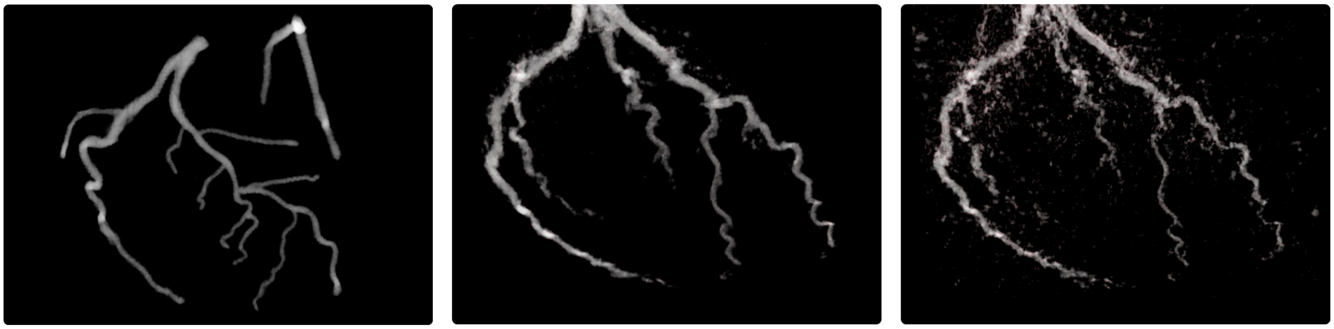

Fig. 3: Volume renderings of the images reconstructed from the CAVAREV data set (a) and the clinical patient data set (b) using spatio-temporal regularization. For the latter, a variant using spatial regularization only is shown for comparison (c).

As for future work, incorporating temporal regularization also into the vessel extraction step—thereby eliminating inconsistencies—might have the potential to further improve image quality in clinical data. Additionally, the method may be extended to cope with respiratory motion, e. g. by strategies based on Fourier-domain or epipolar consistency conditions [9], which are applicable since the extracted vessels are no longer truncated.

Acknowledgments We thank Dr. M. Hell from the University Hospital Erlangen for providing the clinical data. *Disclaimer:* The concepts and information presented in this paper are based on research and are not commercially available.

5. REFERENCES

[1] S. Çimen, A. Gooya, M. Grass, and A. F. Frangi, "Reconstruction of Coronary Arteries from X-ray Angiography: A Review," *Med Image Anal*, vol. 32, pp. 46–68, 2016.

[2] C. Blondel, G. Malandain, R. Vaillant, and N. Ayache, "Reconstruction of coronary arteries from a single rotational X-ray projection sequence.," *IEEE Trans Med Imaging*, vol. 25, no. 5, pp. 653–63, 2006.

[3] H. Wu, C. Rohkohl, and J. Hornegger, "Total Variation Regularization Method for 3-D Rotational Coronary Angiography," in *Bildverarbeitung für die Medizin*, 2011, pp. 434–438.

[4] C. Schwemmer, C. Rohkohl, G. Lauritsch, K. Müller, and J. Hornegger, "Residual Motion Compensation in ECG-Gated Interventional Cardiac Vasculature Reconstruction," *Phys Med Biol*, vol. 58, pp. 3717–3737, 2013.

[5] E. Hansis, D. Schäfer, O. Dössel, and M. Grass, "Projection-based motion compensation for gated coronary artery reconstruction from rotational x-ray angiograms.," *Phys Med Biol*, vol. 53, pp. 3807–20, 2008.

[6] C. Schwemmer, C. Rohkohl, G. Lauritsch, K. Müller, and J. Hornegger, "Opening Windows - Increasing Window Size in Motion-Compensated ECG-gated Cardiac Vasculature Reconstruction," in *Fully3D*, 2013, pp. 50–53.

[7] O. Taubmann, G. Lauritsch, G. Krings, and A. Maier, "Convex temporal regularizers in cardiac C-arm CT," in *CT Meeting*, 2016, pp. 545–548.

[8] C. Rohkohl, G. Lauritsch, A. Keil, and J. Hornegger, "CAVAREV - An Open Platform for Evaluating 3D and 4D Cardiac Vasculature Reconstruction," *Phys Med Biol*, vol. 55, pp. 2905–2915, 2010.

[9] M. Unberath, A. Aichert, S. Achenbach, and A. Maier, "Virtual Single-frame Subtraction Imaging," in *CT Meeting*, 2016, pp. 89–92.

[10] L. Condat, "A generic proximal algorithm for convex optimization – application to total variation minimization," *IEEE Sig Proc Let*, vol. 21, pp. 985–989, 2014.

[11] A. Keil, J. Vogel, G. Lauritsch, and N. Navab, "Dynamic cone-beam reconstruction using a variational level set formulation," in *Fully3D*, 2009.

[12] G.-H. Chen, P. Theriault-Lauzier, J. Tang, B. Nett, S. Leng, J. Zambelli, Z. Qi, N. Bevins, A. Raval, S. Reeder, and H. Rowley, "Time-Resolved Interventional Cardiac C-arm Cone-Beam CT: An Application of the PICCS Algorithm," *IEEE Trans Med Imaging*, vol. 31, pp. 907–923, 2012.

[13] M. Li, H. Kudo, J. Hu, and R. H. Johnson, "Improved iterative algorithm for sparse object reconstruction and its performance evaluation with micro-CT data," *IEEE Trans Nucl Sci*, vol. 51, pp. 659–666, 2004.